# DESIGN, IMPLEMENTATION AND TESTING OF A 24 GHZ 5G BAND RFI DETECTION PAYLOAD FOR A POCKETQUBE

G. Gracia-Sola <sup>1</sup>, S. Podaru <sup>1</sup>, A. Alcantara <sup>1</sup>, A. Garcilla-Morilla <sup>1</sup>, L. Contreras-Benito <sup>1</sup>, A. Perea <sup>1</sup>, A. Camps<sup>1,2,3</sup>

CommsSens Lab, UPC, Dept. of Signal Theory and Communications, BarcelonaTech, 08034 Barcelona.
ASPIRE Visiting International Professor, United Arab Emirates University, CoE, PO Box 15551, Al Ain, UAE.
Institut d'Estudis Espacials de Catalunya IEEC/CTE-UPC, 08034 Barcelona.

### **ABSTRACT**

Due to the recent licensing of the 26 GHz 5G communications bands, the passive microeaves Remote Sensing community is concerned that spurious out-of-band emissions could interfere with the measurements acquired in the 23.8 GHz water vapor resonance band. For this reason, the Frequency Allocations in Remote Sensing (FARS) Technical Committee from the IEEE Geoscience and Remote Sensing Society (GRSS) has procured the development of a RFI monitoring payload to detect possible interferences in the 24 to 25 GHz band. This payload is compatible with the PocketQubes being developed in the framework of the "IEEE GRSS Open PocketQube Kit" educational initiative, and it will be used to measure and determine the occurrence of possible interferences close to the 23.8 GHz water vapor band. This work presents the design, implementation and testing of the 24 to 25 GHz RFI monitoring payload designed for a 1P PocketOube.

*Index Terms*— PocketQubes, Remote Sensing, Radio Frequency Interference, K-band.

### 1. INTRODUCTION

The 23.6-24 GHz band is important to measure water vapor in the Earth's atmosphere for weather forecasts, correcting radar altimeter measurements, etc. [1]. However, the licensing of adjacent bands for the new 26 GHz 5G communications band, specifically from 24.25 GHz to 25.25 GHz, have raised concerns about potential interference from these emissions. This interference could degrade the capabilities of passive Earth Observation measurements and negatively impact meteorological forecasting.

In order to take advantage of the PocketQube being proposed in the "IEEE Open PocketQube Kit", the payload has to be boarded in a 1P PocketQube proposed by the kit, as seen in Fig. 1, requiring minimal modification to the satellite. Each of the PocketQube's has a size of  $50x50x50 \text{ mm}^3$ , an average power consumption of less than 250 mW, and use LoRa for communications [2] [3]. One advantage of the increase in RF frequency is the general reduction in size of the RF components.

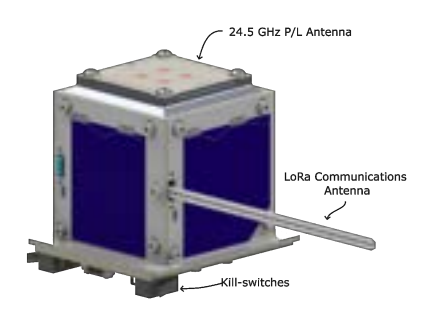


Fig. 1: PocketQube with the K-band RFI monitoring payload.

The PocketQube is designed to be flown in a LEO orbit of an approximated height (h) of 400-500 km. Using an 2x2 patch array antenna, with a beam-width around 40°, the payload will have a footprint of around 360 km. For local applications, the payload could be attached to a drone, with typical maximum flight heights of few hundred meters or less, and a spatial resolution around 200 m.

The payload (Fig. 2) consists of a 2x2 linear patch antenna array tuned at 24.5 GHz with a bandwidth of 1 GHz. A superheterodyne receiver front-end is used to scan the frequency range from 24 GHz to 25 GHz, in 10 MHz channels, and down-converted to 869 MHz, with a gain of around 52 dB. Then, a receiver signal strength indicator (RSSI) provides an output voltage proportional to the sensed RF input power in dB. It also includes an interface module for power supply through the PocketQube power bus and signal conditioning. The power consumption of the payload is around 1 W, which limits its duty cycle in orbit.

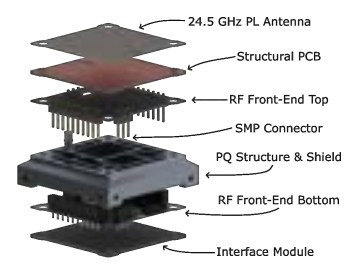


Fig. 2: Exploded view of the K-band RFI monitoring payload.

# 2. INTERFERENCE DETECTION ALGORITHMS FOR A POCKETOUBE

Due to the limited data and power budgets of the PocketQube, the processing of the data generated by the payload has to be performed on-board, and because of the limited computing capabilities of the on-board computer, a reduced subset of the interference detection techniques that appear in the literature can be used [4] [5]. In time-analysis mode, statistical analysis is obtained by retrieving 1000 to 2000 samples from each frequency channel. In frequency analysis mode, all 100 channels are measured, and the power peaks are retrieved.

### 2.1. Pulse and Frequency Thresholding Technique

One simple technique used to determine the possible presence of RFI is to compare temporal or frequency samples of the signal power with a known threshold. The decision is based on the Neyman-Pearson test, that defines a threshold value  $\alpha$  to differentiate between presence (hypothesis  $H_0$ ) or absence (hypothesis  $H_1$ ) of RFI, for a given probability of detection  $(P_D)$  and false-alarm  $(P_{FA})$ , shown in Eq. (1). Both probabilities are related with the likelihood ratio  $(\mathcal{L}(x))$  to obtain a threshold  $(\eta)$  that is defined to achieve the  $P_{FA}$  given the likelihood of the two hypothesis, as seen in Eq. (2).

$$\alpha = P(\mathcal{L}(X) \le \eta | H_0) \tag{1}$$

$$\Lambda(x) = \frac{\mathcal{L}(\mu_0|x)}{\mathcal{L}(\mu_1|x)} \tag{2}$$

### 2.2. Statistical Parameter Analysis

Statistical tests are performed on the measured samples to verify if they belong to a certain known distribution. Because of the output of the RSSI is log-linear, the measurements of the channel (AWGN with absence of RFI) will not follow a Gaussian distribution, but a log-Rayleigh one [6].

Skewness: measures the asymmetry of a random variable distribution around its mean, and is computed with the third central moment (μ<sub>3</sub>) relative to the standard deviation (σ) of the variable, as seen in Eq. (3). If the Skewness results in a value that is different to the expected one for AWG noise, it may imply presence of RFI at the measurement bin.

Skew[X] = 
$$E\left[\left(\frac{X-\mu}{\sigma}\right)^3\right] = \frac{\mu_3}{\sigma^3}$$
 (3)

• **Kurtosis**: measures the "tailness" of the probability distribution of a random varibale, and is computed with the fourth order moment  $(\mu_4)$  related to the standard deviation  $(\sigma)$ , as seen in Eq. (4). A more relevant parameter is the excess-kurtosis, defined as the kurtosis minus

the kurtosis of the known distribution of the channel, since obtaining a value different than 0 would indicate presence of RFI.

$$Kurt[X] = E\left[\left(\frac{X - \mu}{\sigma}\right)^4\right] = \frac{\mu_4}{\sigma^4}$$
 (4)

For random Gaussian variables the skewness is 0, and the kurtosis is 3. However, because the detected signal is in dB (logarithnic) units, these values, and their uncertainty thresholds need to be recomputed accordingly. In addition to skewness and kurtosis the mean and standard deviation of the signals are also computed.

## 3. K-BAND SUPERHETERODYNE RECEIVER FRONT-END

The payload front-end, shown in Fig. 3, consists of a two-stage superheterodyne receiver that amplifies and down-converts the input signal from the antenna to a fixed frequency of 869 MHz for the RSSI, allowing to select between 100 frequency bins of 10 MHz bandwidth each. For any bin, the equivalent noise power assuming a temperature antenna of 290 K is of around -104 dBm. The gain contribution of all the elements in the payload is summarized in Table 1, which added up provide a net gain of 52 dB.

**Table 1**: Front-end components gain summary.

Gain (dB)	Component	Gain (dB)	
+19	LFCW-8000+	-1.5	
-4	SIM-14+	-7	
-10	LEE2-6+	+20.6	
-2	SAW	-3	
+19	LEE2-6+	+20.6	
	+19 -4 -10 -2	+19 LFCW-8000+ -4 SIM-14+ -10 LEE2-6+ -2 SAW	

In a first stage, the input from the antenna is pre-amplified by means of an LNA to reduce the equivalent noise figure of the receiver according to Eq. (5) to around 3.6 dB, and is down-converted using a fixed local oscillator at 17331 MHz to a frequency from 6669 to 7669 MHz, depending on the frequency bin selected. This local oscillator frequency is synthesised by doubling the output frequency of a voltage-controlled oscillator, with an additional gain stage to attack the frequency mixer and reduce the conversion losses. The first stage provides a net gain of 5 dB.

$$F_{\text{Total}} = F_{LNA} + \frac{L_{BPF} - 1}{G_{LNA}} + \frac{L_{Mixer} - 1}{G_{LNA}L_{BPF}}$$
 (5)

The second stage down-converts the variable band into a fixed intermediate frequency of 869 MHz with a local oscillator controlled by the on-board computer that can sweep the

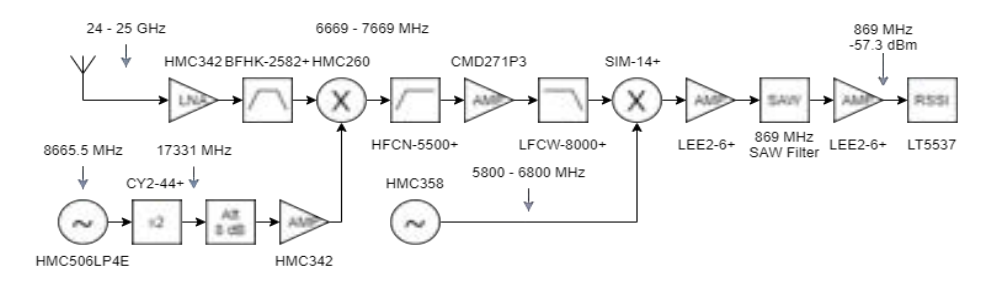


Fig. 3: Block Diagram of the RFI detection payload.

band from 5800 to 6800 MHz. The bin selection is achieved by means of a SAW filter of 10 MHz bandwidth centered at that intermediate frequency. This stage also adds a net gain of 46.7 dB. Finally, a matching network is used to increase the sensitivity of the LT5537 RSSI used to detect the RF power.

Thus, the frequency bin can be selected according to Eq. (6), and the output voltage of the RSSI in function of the frontend input power is expressed as Eq. (7).

$$f_{\rm bin} = f_{\rm LO1} + f_{\rm LO2} + 869 = 18369 + f_{\rm LO2} \quad [{\rm MHz}] \quad (6)$$

$$V_{RSSI} = 31.4 \cdot 10^{-3} (P_{FEin[dBm]} + 50) + 2.6$$
 [V] (7)

Each front-end stage is located in a different board, shown in Fig. 4, and are supported by a metallic structure that includes enclosures for each different frequency part to increase isolation, and is also used as the main structural part of the PocketQube. An interface board is added in order to provide all the needed power supplies, and to condition the analog signals for the payload. The overall power consumption of the front-end is around 900 mW, which is significantly higher than the power generated by the PocketQube. Therefore, the payload must be duty cycled.

### 4. 2X2 PATCH ANTENNA ARRAY DESIGN

The antenna consists of a 2x2 square patch array, shown in Fig. 5, centered at 24.5 GHz that with a 1 GHz bandwidth and matching  $(S_{11})$  below -10 dB, shown in Fig. 6. It is manufactured in a RO5880 substrate that makes the design feasible thanks to the low  $\mathcal{E}_r$  value of 2.2, and with 0.254 mm thickness to obtain the desired bandwidth. This substrate also

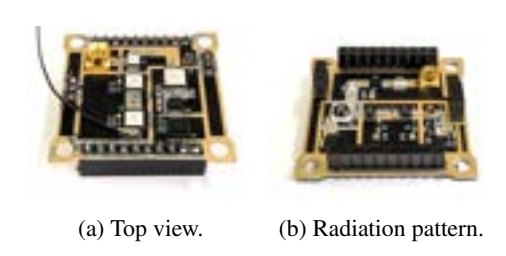


**Fig. 4**: Picture of top (Fig. 4a) and bottom (Fig. 4b) stages of the RF front-end.

increases the antenna efficiency thanks to its low tangent of losses, and reduces the variability due to the small variation of  $\mathcal{E}_r$ .

Each radiating element is a micro-strip square patch with an inset feed for matching, designed to have a input impedance of  $50~\Omega$  using (8), where R is the depth of the inset feed and L is the height of the patch. For simplicity, the array has been designed with linear polarization, and has a  $180^{\circ}$  phase shift between each pair of patches. The design has been optimized by simulation using CST to fulfill the specifications, which yields to beam-width of  $31.3~^{\circ}$ , a directivity of  $13~\mathrm{dB}$ , and with the side-lobes at  $-12.2~\mathrm{dB}$ .

$$Z_{in}(R) = \cos^4\left(\frac{\pi R}{L}\right) Z_{in}(0) \tag{8}$$

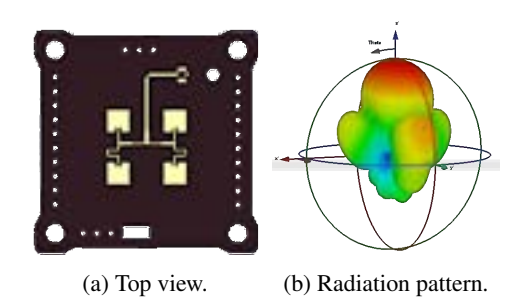
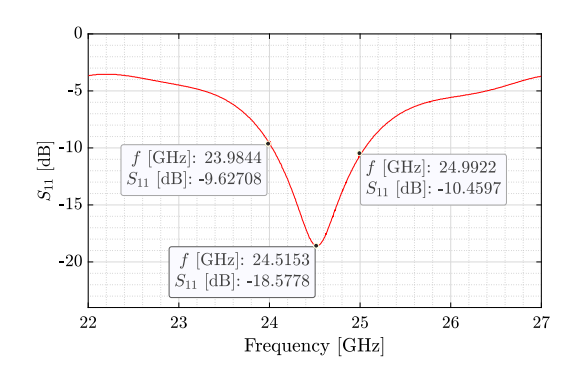
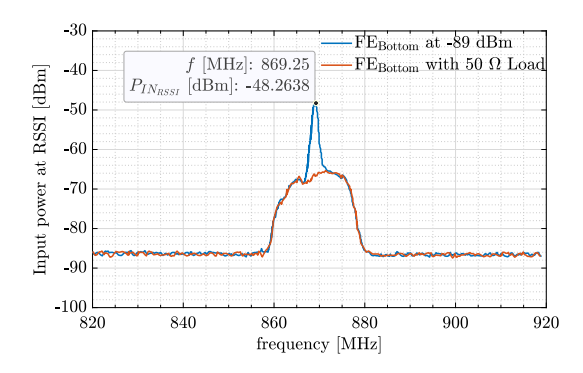


Fig. 5: 2x2 patch antenna array, and radiation pattern.



**Fig. 6**:  $S_{11}$  simulation of the 2x2 patch antenna array.



**Fig. 7**: Output spectrum of the front-end bottom stage for two inputs: tone of -89 dBm and 6869 MHz (blue), and  $50~\Omega$  load.

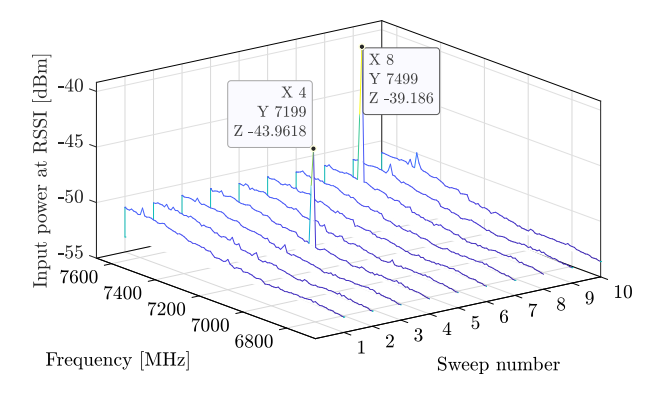


Fig. 8: Waterfall measurements with simulated RFI.

### 5. TESTING AND RESULTS

The tests of the second front-end stage, presented in Fig. 7, have been conducted tuning the LO at 6000 MHz and for two different inputs: a -89 dBm tone at 6869 MHz, and a 50  $\Omega$  load. The second stage is able to down-convert the RF input signal into the desired intermediate frequency of 869 MHz, and shows the selective behaviour of the payload thanks to the SAW filter. Considering the pass-band at -6 dB for higher selectivity, the stage has a bandwidth of 16 MHz. Moreover, the stage provides a gain of 40 dB, which is smaller than the desired 46.7 dB.

To test the automatic behavior of the payload, several frequency sweep iterations have been performed to obtain a waterfall graph, ilustrated in Fig. 8. For this test, the bins are separated by 10 MHz, and two different tones of -85 dBm have been input at different instances with the objective of simulating possible RFI: first at 7200 MHz and after at 7500 MHz. The test shows that the 2 tones can be identified with success, with an error in the power level coming from a slight increase in gain at higher frequencies, that has to be calibrated.

### 6. CONCLUSIONS

The tests performed to the K-band RFI monitoring payload show that it provides the desired behavior at ambient environmental conditions. A calibration of the final version of the payload will be needed to compensate unforeseen variations of both gain and frequency performances. The full payload and the antenna array test results will be presented at the conference, and a drone test campaign will follow to validate the payload operation with real measurements.

#### 7. ACKNOWLEDGMENTS

This work was sponsored by the Frequency Allocations in Remote Sensing (FARS) Technical Committee of the IEEE Geoscience and Remote Sensing Society (GRSS).

This project was also sposored in part by the project "GENESIS: GNSS Environmental and Societal Missions – Subproject UPC", Grant PID2021-126436OB-C21 funded by the Ministerio de Ciencia e Investigación (MCIN)/Agencia Estatal de Investigación (AEI)/10.13039/501100011033 and EU FEDER "Una manera de hacer Europa".

### 8. REFERENCES

- [1] Thomas J. Kleespies, "Relative information content of the advanced technology microwave sounder and the combination of the advanced microwave sounding unit and the microwave humidity sounder," *IEEE Transactions on Geoscience and Remote Sensing*, vol. 45, no. 7, pp. 2224–2227, 2007.
- [2] A. Camps, S. Podaru, D. Llaveria, G. Gracia-Sola, and A. Alcantara, "The 'open pocketqube kit': an ieee grss educational initiative," *IEEE Geoscience and Remote Sensing Magazine*, vol. 5, no. 2, pp. 4–6, 6 2017.
- [3] Alba Orbital, TUDelft, and Gauss, "The PocketQube Standard, Issue 1," http://www.albaorbital.com/pocketqube-standard, June 2018, (Last viewed April 2023).
- [4] A. Perez, JF. Munoz-Martin, J. Querol, H. Park, and A. Camps, "Implementation of a testbed for gnss-r payload performance evaluation," *IEEE Journal of Selected Topics in Applied Earth Observations and Remote Sens*ing, vol. 13, pp. 2708–2715, 2020.
- [5] J. Querol, Radio frequency interference detection and mitigation techniques for navigation and Earth observation, Ph.D. thesis, Polytechnic University of Catalonia, Spain, 2018.
- [6] B. Rivet, L. Girin, and C. Jutten, "Log-rayleigh distribution: A simple and efficient statistical representation of log-spectral coefficients," vol. 15, pp. 796–802, 2007.